Allyson Tessin

Isotopically depleted carbon in the mid-depth South Atlantic during the last deglaciation

Submitted for Publication in:

Paleoceanography

in lieu of thesis in partial fulfillment of the requirements for the degree of
Master of Science in Earth and Environmental Sciences
Department of Earth and Environmental Sciences
The University of Michigan

Accepted by:

Signature	Name	Date
Signature	David Lund	4/11/13
Signature	Ingrid Hendy	4/12/13
Rebecca Lange (Department Chair Signature)	Rebecca Lange	4/15/13

Author Signature

Earth and Environmental Sciences
UNIVERSITY OF MICHIGAN

Isotopically depleted carbon in the mid-depth South Atlantic during the last deglaciation

A. C. Tessin and D. C. Lund
Department of Earth and Environmental Sciences
University of Michigan
Ann Arbor, MI USA

Abstract

The initial rise in atmospheric CO_2 during the last deglaciation was likely driven by input of carbon from a ^{13}C-depleted reservoir (Schmitt et al., 2012). Here we show that high resolution benthic foraminiferal records from the mid-depth Brazil Margin display an abrupt drop in $\delta^{13}C$ during Heinrich Stadial 1 (HS1) that is similar to but larger than in the atmosphere. Comparing the Brazil Margin results to published records from the North Atlantic, we are unable to account for the South Atlantic $\delta^{13}C$ data with conservative mixing between northern and southern component watermasses. Rapid input of abyssal water from the Southeast Atlantic could account for deglacial $\delta^{13}C$ anomalies at the Brazil Margin but it would require a reversal in deep water flow direction compared to today. A new mid-depth watermass may explain similar HS1 $\delta^{13}C$ values in both the North and South Atlantic, but contrasting oxygen isotopic values between the two basins do not support the presence of a single dominant watermass at mid-depths. Instead, it appears that $\delta^{13}C$ behaved non-conservatively during the deglaciation, possibly reflecting the input of carbon from an isotopically depleted source.

Introduction

The rise in atmospheric carbon dioxide between the Last Glacial Maximum (LGM) and the Holocene was first recognized over 30 years ago (Neftel et al., 1982) yet the underlying mechanisms responsible for the CO_2 change remain unclear (Sigman and Boyle, 2000; Sigman et al., 2010). High resolution ice core records indicate that the initial 30 ppmv increase in CO_2 from ~17 to 16 kyr BP coincided with a decrease in the $\delta^{13}C$ of atmospheric CO_2 of 0.3‰ (Schmitt et al., 2012). The synchroneity of the signals suggests the release of carbon from a ^{13}C-depleted reservoir into the atmosphere was a key initiator of the last deglaciation.

Carbon isotope minima were widespread phenomena in the surface and mid-depth ocean during the last deglaciation (Oppo and Fairbanks, 1989; Ninnemann and Charles, 1997; Spero and Lea, 2002; Curry et al., 1988; Peck et al., 2007). The largest $\delta^{13}C$ anomalies occurred in the mid-depth North Atlantic. South of Iceland, $\delta^{13}C$ decreased by ~1‰ at water depths from 1200 m to 2300 m (McManus et al., 1999; Rickaby and Elderfield, 2005; Thornalley et al., 2010). Similar anomalies occurred at 1300 m water depth in the western tropical Atlantic (Zahn and Stuber, 2002) and 1100 m in the eastern subtropical Atlantic (Zahn et al., 1997). A variety of mechanisms have been proposed to explain the carbon isotope minima, including regional brine formation (Dokken and Jansen, 1999; Thornalley et al., 2010; Waelbroeck et al., 2011), greater incursion of southern source intermediate water (Rickaby and Elderfield, 2005), and weakening of the Atlantic meridional overturning circulation (Zahn et al., 1997). The latter mechanism appears to be consistent with evidence for reduced export of Pa from the North Atlantic during the deglaciation relative to the LGM (Gherardi et al., 2009).

The Brazil Margin cores used in this study are ideally located to evaluate the evolution of Atlantic watermasses from the LGM to the Holocene. In the modern Southwest Atlantic, the cores span the transition between Antarctic Intermediate Water (AAIW), Upper Circumpolar Deep Water (UCDW), and North Atlantic Deep Water (NADW) (Figure 1). During the LGM, the core locations were influenced by Glacial Antarctic Intermediate Water (GAAIW), Glacial North Atlantic Intermediate Water (GNAIW), and Glacial Antarctic Bottom Water (GAABW) (Curry and Oppo, 2005). Below we show that the Brazil Margin $\delta^{13}C$ time series display a negative excursion similar to the record of atmospheric $\delta^{13}C$ during the deglaciation. We then discuss whether the Brazil Margin data can be explained by conservative mixing between northern and southern waters.

Methods

The analyses presented in this paper are based on 6 cores from 1200 m to 2500 m water depth that were retrieved during the KNR159-5 cruise to the Brazil Margin (Curry and Oppo, 2005). Cores discussed in this paper include 36GGC, 17JPC, 78GGC, 33GGC, 42JPC, and 30GGC (Table 1). Each core was sampled at 4 or 5 cm intervals and the resulting samples were then freeze-dried, washed through a 150 μm sieve, and dried at 40°C.

Radiocarbon

Planktonic foraminifera (*G. ruber* and *G. sacculifer*) were picked from the >250 μm size fraction of each sample for accelerator mass spectrometry (AMS) radiocarbon dates. Radiocarbon dating was carried out at the KCCAMS laboratory at University of California, Irvine, where the samples underwent a 10% leach using 0.01 N HCl to ensure removal of any modern ^{14}C. The foraminifera were then hydrolyzed in 85% phosphoric acid and the resulting CO_2 was combined with hydrogen and iron powder at 560˚C to create graphite. The graphite was analyzed using AMS to obtain ^{14}C results.

Modern reservoir ages along the coast of southeastern Brazil are 407±59 years (1σ), equivalent to a ΔR of 7±59 years (Angulo et al., 2005). For age calibration purposes, we used a ΔR 0±200 years (1σ) to account for unknown changes in reservoir age in the geologic past. Calendar ages were calibrated using Calib v.6.0 (http://calib.qub.ac.uk/calib/). The uncertainties in calibrated calendar ages, typically ±300 years (1σ), are due primarily to our assumed uncertainty in ΔR.

Stable isotopes

Benthic stable carbon and oxygen isotopic analyses were based on individual tests of *Cibicidoides* species from the >250 μm size fraction. Analyses were run on a Finnigan MAT 253 triple-collector gas source mass spectrometer coupled to a Finnegan Kiel automated carbonate device at the University of Michigan's Stable Isotope Laboratory. Samples for cores 42JPC and 36GGC were run at Woods Hole

Oceanographic Institution (Oppo and Horowitz, 2000; Curry and Oppo, 2005). Isotope values at Michigan were corrected to Vienna Pee Dee Belemnite (VPDB) using NBS 19 (n =78, $\delta^{13}C$ = 1.94 ± 0.04‰, $\delta^{18}O$ = -2.19 ± 0.07‰) and NBS 18 (n = 12; $\delta^{13}C$ = -5.00 ± 0.04‰, $\delta^{18}O$ = -22.98 ± 0.06 ‰).

In addition to NBS 18 and NBS 19, we used the Atlantis II standard ($\delta^{18}O$ = 3.42‰; Ostermann and Curry, 2000) to constrain the 'heavy' end of the oxygen isotope spectrum. Atlantis II standards run during this study yield a mean $\delta^{18}O$ of 3.47 ± 0.08‰ (n = 90), within one-sigma error of the 3.42‰ value presented in Ostermann and Curry (2000). Atlantis II $\delta^{18}O$ values run during analysis of samples for core 17JPC averaged 3.52‰. In this instance, we subtracted 0.1‰ from the unknowns to compensate for the higher than normal Atlantis II results.

Results

Age Models

Age models for 17JPC, 78GGC, 33GGC, and 30GGC are shown in Figure 2. The age models for 36GGC and 42JPC are presented in Sortor and Lund (2011) and Hoffman and Lund (2012), respectively. Each core has sedimentation rates of 2-3 cm/kyr during the Holocene with higher rates during the deglaciation and LGM, ranging from 5 cm/kyr to 35 cm/kyr (Figure 2). The high accumulation rates for 78GGC and 33GGC suggest the core locations were sediment drift sites during the deglaciation and LGM. The cores generally lack modern core tops, with the most recent material dating to between 0.5 kyr BP and 3 kyr BP. Non-zero core top ages may be due to a lack of sediment deposition, erosion by deep currents, or an artifact of the coring process.

The radiocarbon results illustrate clear age reversals in cores 78GGC, 17JPC and 30GGC. Deglacial age reversals have been documented in other cores from the Brazil Margin; Sortor and Lund (2011) used stable isotopic data to conclude that reversals in 36GGC were due to deep burrowing. A similar phenomenon appears to have occurred in 78GGC, where anomalously low benthic $\delta^{18}O$ values from 69 cm to 81 cm coincide with an interval of unusually young radiocarbon ages (Figure 3). The anomalous $\delta^{18}O$ points have values ranging from 3.5‰ to 3.7‰, indicating they originated from the 35 cm to 45 cm stratigraphic interval. Radiocarbon ages of ~13.5 kyr BP in the disturbed section support this interpretation. We exclude these data from the age model for 78GGC. Note that the section of the core with the large decline in $\delta^{13}C$ (discussed below) occurs prior to the disturbed section. Two additional isolated reversals prior to HS1 (at 145 cm and 165 cm) are also excluded from the age model for 78GGC (Figure 2b).

In the case of 30GGC, there are two possible age models; one that includes the age at 41 cm and one that excludes it (Figure 2d). This age is not a reversal *per se* but would require a drastic change in sedimentation rate. Since there is a clear reversal at 39 cm, we chose to use the age model that excludes both points (dashed black line). Large age reversals in 17JPC at 50 cm, 58 cm, 66 cm, and 82 cm were excluded from the age model for this core. Age models for 78GGC, 17JPC and 30GGC were produced by linear interpolation between the remaining calendar ages. Age inconsistencies in 33GGC are subtler than the other cores; many are within error of adjacent dates in the stratigraphy (Figure 2c). As a result, we used a polynomial fit to construct the age model rather than linear interpolation between individual radiocarbon control points.

Stable isotopic time series

Benthic foraminiferal $\delta^{18}O$ time series for the Brazil Margin are shown in Figure 4. The contrast between LGM and Holocene $\delta^{18}O$ values is ~2.0‰ at water depths below 2000 m compared to ~1.8‰ above 2000 m, consistent with results spanning the full water column range at the Brazil Margin (Curry and Oppo, 2005; Lund et al., 2011). The new radiocarbon-constrained records indicate the timing of the LGM to Holocene shift varies by water depth (Figure 4). Above 2200 m, benthic $\delta^{18}O$ begins to decrease at 17.5-18.0 kyr BP whereas below 2200 m, the $\delta^{18}O$ decrease occurs after 17.0 kyr BP, similar to the depth-dependent timing noted at other Atlantic sites (Waelbroeck et al., 2011).

Benthic $\delta^{13}C$ in the deepest cores (2300-2500 m) and shallowest core (1300 m) increase by 0.5-0.8‰ between the LGM and Holocene, while those in between (1800-2100 m) show little glacial-interglacial difference (Figure 4). The most striking feature of the $\delta^{13}C$ records is the pronounced negative excursion near the beginning of Heinrich Stadial 1 (HS1; 14.5-17.5 kyr BP). The decrease is largest between 1600 m to 2100 m water depth (~0.5‰), with smaller excursions at 2300 m and 2500 m (~0.2‰). The one exception where $\delta^{13}C$ increased monotonically during the deglaciation is at 1300 m water depth.

The two high resolution records at 1800 m and 2100 m have $\delta^{13}C$ histories similar to the atmosphere (Figure 5). Each record displays a pattern of change that resembles a leaning 'W', including an abrupt drop in $\delta^{13}C$ near ~18 kyr BP, a partial recovery by 14 kyr BP, a modest decrease at 12-13 kyr BP, and finally a gradual increase into the mid-Holocene. The magnitude of the oceanic $\delta^{13}C$ anomalies is ~0.2‰ larger than in the atmosphere. For each benthic $\delta^{13}C$ record the maximum rate of decline occurs at 17.8 kyr BP, assuming the regional offset in surface water reservoir age (ΔR) was 0±200 years (1σ) during the LGM and deglaciation (Figure 5). If instead ΔR was 400 years, the maximum rate of $\delta^{13}C$ change occurs at 17.3 kyr BP. By comparison, the maximum rate of $\delta^{13}C$ change in the atmosphere occurs between 16.9 kyr BP and 17.3 kyr BP. If the age models for these records are correct, it appears that the rapid decrease in $\delta^{13}C$ at the Brazil Margin either led or was synchronous with the atmosphere.

Discussion

The strong correspondence between the Brazil Margin and atmospheric $\delta^{13}C$ records suggests they are linked by a common mechanism. One possibility is that the Brazil Margin $\delta^{13}C$ anomalies reflect changes in the composition of northern component water or its proportion relative to southern component water.

Alternatively, input of abyssal water from the South Atlantic could have driven the $\delta^{13}C$ signal. In either case, the apparent changes in circulation represented by the benthic $\delta^{13}C$ records must have also led to outgassing of ^{13}C-depleted carbon from the ocean in such a way that both the oceanic and atmospheric $\delta^{13}C$ records had similar variability. Below we first review LGM watermass properties at the Brazil Margin to provide context for the deglaciation. We then evaluate the different circulation mechanisms that could potentially account for the deglacial anomalies.

LGM watermass proportions

During the LGM, Brazil Margin $\delta^{18}O$ and $\delta^{13}C$ pairs from 1800 m to 4000 m water depth fall on a mixing line between GNAIW and GAABW (Figure 6a). Assuming $\delta^{13}C$ values of 1.4‰ for GNAIW (Curry and Oppo, 2005) and -0.2‰ for GAABW (Hoffman and Lund, 2012), the $\delta^{13}C$ results at 1800 m can be explained by a mixture of 25% GAABW and 75% GNAIW (Table 2). Given that $\delta^{13}C$ is a non-conservative tracer, it is important to validate these proportions using $\delta^{18}O$. We do so by estimating the predicted $\delta^{18}O$ at each depth given the $\delta^{13}C$-based proportions and the $\delta^{18}O$ endmember values for GNAIW and GAABW. Using an $\delta^{18}O$ of 4.2‰ for GNAIW (Curry and Oppo, 2005) and 4.9‰ for GAABW (Hoffman and Lund, 2012), the predicted $\delta^{18}O$ at 1800 m is 4.38‰, indistinguishable from observed value of 4.40‰ (Table 2). The predicted and observed LGM $\delta^{18}O$ values at 2100 m, 2300 m, and 2500 m are also in good agreement.

Between 1100 m and 1600 m, the isotopic data generally fall between GNAIW and GAAIW (Figure 6a). Water at 1600 m depth is composed of ~50% GAAIW and ~50% GNAIW while water at 1300 m appears to consist largely of GAAIW. The offset between observed and estimated $\delta^{18}O$ for the shallower cores is larger than for the deeper sites (Table 2). This is mostly likely due to the small contrast in $\delta^{18}O$ values for GAAIW (4.3‰) and GNAIW (4.2‰) relative to the uncertainty in mean LGM values at each water depth (±0.05‰). Nevertheless, the Brazil Margin data suggest that $\delta^{13}C$ at mid-depths acted as a largely conservative tracer during the LGM, consistent with results from deeper in the water column (Hoffman and Lund, 2012).

Northern component influence during HS1

An apparent reorganization in watermass structure occurred during HS1 (Figure 6b). Between 1800 m to 2300 m water depth, $\delta^{18}O$ decreased 0.4-0.6‰ while $\delta^{13}C$ decreased 0.2-0.5‰. In comparison, $\delta^{18}O$ of southern component water (SCW) decreased by ~0.2‰ while its $\delta^{13}C$ increased ~0.2‰ (Hoffman and Lund, 2012). Northern component water (NCW) underwent the largest isotopic shift during HS1, with $\delta^{18}O$ and $\delta^{13}C$ decreasing by ~1.0‰ and ~0.7‰, respectively. Assuming HS1 end member $\delta^{18}O$ values of 3.1‰ for NCW and 4.6‰ for SCW, the HS1 results from 1800 m to 2300 m water depth can be explained by a mixture of approximately 60% SCW and 40% NCW. Compared to the LGM proportions (Table 2), this represents a substantial reduction in the influence of NCW at the Brazil Margin. Unlike the LGM, however, the HS1 $\delta^{18}O$-$\delta^{13}C$ pairs do not fall on a mixing line between NCW and SCW. Projecting HS1 $\delta^{18}O$ values to the mixing line, we estimate that $\delta^{13}C$ for the mid-depth Brazil Margin sites should range from 0‰ at 2500 m to 0.3‰ at 1300 m, about 0.2-0.4% lower than observed (Figure 6b).

Given that the Atlantic circulation was probably not in steady state during the deglaciation, a full accounting of isotopic records in the Southwest Atlantic should consider transient changes in NCW and SCW. Unfortunately, surface water reservoir age variability of up to several hundred years at the South Atlantic and more than 1000 years in the North Atlantic (Waelbroeck et al., 2001) precludes reliable quantification of the effect of transient endmember variability on the mid-depth isotopic records from the Brazil Margin.

Input of abyssal water

The $\delta^{13}C$ results in Figure 4 imply that water depleted in ^{13}C invaded the mid-depth South Atlantic during the deglaciation. Because the abyssal Southwest Atlantic was characterized by low $\delta^{13}C$ during the LGM, input of water from the abyss could account for the abrupt changes at mid-depth. The flow path would presumably involve upwelling south of the Antarctic Polar Front (Marshall and Speer, 2012; Anderson et al., 2009) and the subsequent formation and northward advection of a new mid-depth watermass. Just prior to HS1, GAABW in the Brazil Basin had a $\delta^{13}C$ of -0.2±0.2‰ (Hoffman and Lund, 2012). Accounting for the HS1 $\delta^{13}C$ excursions would require 40±10% of the water at mid-depth to be replaced by GAABW, assuming no dilution by mixing during its transit to the Brazil Margin.

Input of GAABW would also influence benthic foraminiferal $\delta^{18}O$. During the LGM, GAABW had an $\delta^{18}O$ of 4.9±0.1‰ (Hoffman and Lund, 2012). Rapid addition of 40±10% GAABW would cause $\delta^{18}O$ to increase by 0.2±0.05‰, yet the records at 1800 m and 2100 m instead show either no change or a small decrease from the LGM to HS1 (Figure 7). If GAABW was the source of the $\delta^{13}C$ anomalies, the associated $\delta^{18}O$ signal must have been offset by warming or the input of ^{18}O-depleted water from the surface ocean.

Results from the Cape Basin suggest abyssal water in the Southeast Atlantic had a $\delta^{13}C$ of -0.9±0.1‰ and $\delta^{18}O$ of 4.2±0.1‰ (Ninnemann and Charles, 2002; Waelbroeck et al., 2011). Although benthic $\delta^{13}C$ in this region may be influenced by epibenthic decay of organic matter (Mackensen et al., 1993) and the $\delta^{18}O$ results may be biased by laboratory calibration issues (Ostermann and Curry, 2000; Hodell et al., 2003), the potential influence of this isotopically distinct watermass must also be considered. Accounting for the Brazil Margin $\delta^{13}C$ anomalies would require ~25% of the water at mid-depths to originate from the Southeast Atlantic. Adding this proportion would cause only a slight (<0.1‰) decrease in $\delta^{18}O$, consistent with observations (Figure 7). However, the net advective flow at 1-3 km water depth in the modern South Atlantic is eastward from the Brazil Basin to the Cape Basin, followed by entrainment in the Antarctic Circumpolar Current (ACC) (Sloyan and Rintoul, 2001). Assuming a similar circulation pattern during the deglaciation, the isotopic signal would need to be transmitted from the Southeast Atlantic via the ACC around Antarctica with little or no dilution by mixing. Although we cannot rule out this possibility, it appears to be an unlikely explanation of the large and abrupt $\delta^{13}C$ signals at the Brazil Margin.

A new mid-depth watermass

Carbon isotopic results from the North and South Atlantic suggest a single ^{13}C-depleted watermass occupied mid-depths during HS1. In the western tropical North Atlantic, a region where large changes in reservoir age are unlikely, $\delta^{13}C$ dropped abruptly at approximately 18 kyr BP, reached a minimum value of ~0.6‰ during HS1, and then recovered slowly into the mid-Holocene (Zahn and Stuber, 2002) (Figure 8). This pattern is very similar to that observed at the Brazil Margin. Homogeneous $\delta^{13}C$ values are observed throughout the mid-depth western Atlantic during HS1 (Oppo and Curry, 2012). Indeed, vertical profiles from the North and South Atlantic show that the mid-depth records are characterized by a $\delta^{13}C$ of 0.6±0.1‰ (Figure 9). This pattern is strikingly different than the LGM where the clear north-south contrast in $\delta^{13}C$ reflects the dominant influence of GNAIW in the North Atlantic. In the South Atlantic, GNAIW manifests itself as $\delta^{13}C$ maximum near 1800 m water depth (Figure 9).

Unlike $\delta^{13}C$, benthic $\delta^{18}O$ profiles from the North and South Atlantic are very different during HS1. At the Brazil Margin, $\delta^{18}O$ ranges from 3.8‰ at 1300 m to 4.5‰ at 2500 m (Figure 9). In the North Atlantic, $\delta^{18}O$ values are lower throughout the same depth interval, spanning from 3.1‰ to 4.1‰. At the Brazil Margin, HS1 $\delta^{18}O$ values decreased by 0.1‰ to 0.5‰ relative to the LGM whereas in the North

Atlantic the $\delta^{18}O$ decrease is much larger, ranging from 0.5‰ to 1.0‰. The results suggest the $\delta^{18}O$ anomaly originated in the North Atlantic, perhaps due to influx of ^{18}O-depleted melt water. The different $\delta^{18}O$ histories in the two basins are also apparent in the time series in Figure 8. Throughout the LGM and deglaciation, benthic $\delta^{18}O$ in the western tropical Atlantic is consistently 0.5‰ to 0.8‰ lower than at the Brazil Margin even though the $\delta^{13}C$ history in the two locations is nearly identical. The $\delta^{18}O$ data highlight the existence of two separate watermasses at mid-depth, in contrast to the $\delta^{13}C$ results. Given that $\delta^{18}O$ is a conservative watermass tracer (Lund et al., 2011), it appears that another process is necessary to account for the $\delta^{13}C$ minima.

What could cause a similar $\delta^{13}C$ history in the North and South Atlantic? Air-sea gas exchange with a ^{13}C-depleted atmosphere would cause the $\delta^{13}C$ in the source regions for northern and southern component water to decrease. If this were the case, the signal must have somehow been amplified given the larger oceanic $\delta^{13}C$ anomaly (Figure 5). Temperature-driven amplification (e.g. Broecker and Maier-Reimer, 1992) is unable to account for the larger oceanic change because such a process would yield opposite $\delta^{13}C$ signals in the ocean and atmosphere (Spero and Lea, 2002; Ninnemann and Charles, 1997).

The timing of the Brazil Margin $\delta^{13}C$ anomalies also appears to be inconsistent with an atmospheric driver. The mean ventilation age at 2000 m water depth in the modern Southwest Atlantic is approximately 400 years (Gebbie and

Huybers, 2012). If enhanced Southern Ocean upwelling and formation of a new watermass created the $\delta^{13}C$ minima, the shift in atmospheric $\delta^{13}C$ should lead mid-depth records by several hundred years. Instead, the oceanic records appear to lead or be synchronous with the atmosphere (Figure 5). An increase in surface ocean ΔR at the Brazil Margin in excess of 500 years is necessary for the atmosphere to feasibly lead the oceanic signal. Large shifts in ΔR seem unlikely at the latitude of the Brazil Margin where subtropical convergence results in a modern ΔR of 0 years (Angulo et al., 2005). Given age model uncertainties, establishing the exact phasing of the atmospheric $\delta^{13}C$ relative to 2000 m water depth will require the development of high-resolution planktonic $\delta^{13}C$ records from the Brazil Margin. Regardless of the relative timing, the magnitude of the oceanic anomalies indicates the atmosphere was not the primary driver of common $\delta^{13}C$ variability in the North and South Atlantic.

Non-conservative behavior of $\delta^{13}C$

Our discussion of watermasses during the LGM and HS1 is based on the assumption advection and diffusion are the primary factors that influence benthic foraminiferal $\delta^{13}C$. Although benthic $\delta^{13}C$ at the Brazil Margin acted conservatively during the LGM and Holocene (Hoffman and Lund, 2012), it may have acted non-conservatively during the deglaciation. The enigmatic nature of the Brazil Margin isotopic results and the apparent ubiquity of the HS1 $\delta^{13}C$ anomaly in the Atlantic suggest that another source of carbon may have been involved. Biological remineralization of marine organic carbon is an unlikely culprit because it would cause $\delta^{13}C$ to be lower than expected from watermass mixing rather than higher (Figure 6). Evaluating other potential carbon sources will require high-resolution reconstructions from a range of locations to determine whether the isotopic anomalies are consistent with an alternative reservoir.

Conclusions

Mid-depth benthic foraminiferal records from the Brazil Margin display abrupt negative $\delta^{13}C$ anomalies similar to the atmosphere during the last deglaciation. The magnitude of the Brazil Margin $\delta^{13}C$ signal is larger than in the atmosphere, similar to the pattern in published $\delta^{13}C$ records from the North Atlantic. These findings strongly point towards the ocean as a source of the deglacial atmospheric $\delta^{13}C$ anomaly.

Broadly speaking, the coherence between the Brazil Margin and atmospheric $\delta^{13}C$ records can be explained in one of two ways. One possibility is that changes in the oceanic circulation simultaneously altered the watermass distribution in the Southwest Atlantic and influenced the outgassing of ^{13}C-depleted carbon from the abyssal ocean. Alternatively, input of ^{13}C-depleted carbon from another source could have moved both the upper ocean and atmosphere towards more depleted values. We evaluate the first possibility by comparing the Brazil Margin results with stable isotopic constraints for Atlantic watermasses during the LGM and HS1. During the LGM, stable isotopic results from mid-depths can be explained in terms of conservative mixing between northern and southern component waters.

During HS1, however, we are unable to easily account for the Brazil Margin results with a simple two endmember mixing model. A new mid-depth watermass characterized by low $\delta^{13}C$ is apparently required.

Given that GAABW had low $\delta^{13}C$ values during the LGM, it is logical invoke input of water from the abyss as a source ^{13}C-depleted water. By mass balance, the $\delta^{13}C$ anomalies would require a large fraction of the water at mid-depths to be pure GAABW from the Southwest Atlantic. Input of this quantity of GAABW would also cause $\delta^{18}O$ to increase, yet little change is observed. The influence of GAABW could be minimized via warming or the input of ^{18}O-depleted water, but it is unlikely that such compensation would perfectly offset the abyssal signal. Water from the deepest Southeast Atlantic could be a feasible source of low $\delta^{13}C$ but the flow path required (from the Cape Basin to the Brazil Basin) is opposite that observed in the modern South Atlantic.

Input of abyssal water may help explain the Brazil Margin results but it does little to reconcile conflicting stable isotope data in the North and South Atlantic. Similar absolute $\delta^{13}C$ values throughout the Atlantic imply that a single watermass dominated the mid-depths during HS1. However, $\delta^{18}O$ results from the same cores show a strong meridional gradient in $\delta^{18}O$, with isotopically depleted values in the north and comparatively enriched values to the south. Given that $\delta^{18}O$ is a conservative tracer, these data suggest two distinct watermasses influenced the mid-depth Atlantic during HS1. Benthic foraminiferal $\delta^{13}C$, on the other hand, is a non-conservative tracer that is influenced by advection, diffusion, and the input of carbon from other sources. Given that biological remineralization of marine organic matter does not appear to be a viable explanation of the $\delta^{13}C$ anomalies, it appears that another source of carbon external to the ocean-atmosphere system may have been involved.

Acknowledgements

We would like to thank Lora Wingate for technical assistance in producing the stable isotope results presented here. We are also grateful to John Southon for his oversight of the radiocarbon analyses. We would like to thank Jamie Hoffman, Rachel Franzblau, Rachel Seltz, and Elliot Jackson for sample processing. We are grateful to the WHOI core lab for sample collection and archiving and to Bill Curry and Delia Oppo for the opportunity to work on the Brazil Margin cores. This work was supported by NSF grant OCE-1003500.

Figure captions:

Figure 1

Locations of cores used in this paper superimposed on the phosphate concentration of the World Ocean Circulation Experiment (WOCE) A16 section in the Atlantic Ocean (Schlitzer et al., 2000). The Brazil Margin cores at 27°S span Antarctic Intermediate Water (AAIW), Upper Circumpolar Deep Water (UCDW), and North Atlantic Deep Water (NADW). Also shown are core locations for NEAP 4K (Rickaby and Elderfield, 2005), RAPiD 10-1P, RAPiD 15-4P and RAPiD 17-5P (Thornalley et al., 2010), SO75-26KL (Zahn et al., 1997), M35003 (Zahn and Stuber, 2002), and MD01-2461 (Peck et al., 2007).

Figure 2

Calendar ages (red circles) and age models (dashed lines) for cores 17JPC, 78GGC, 33GGC, and 30GGC. Error bars for each calendar age represent the ±1σ uncertainty. Age reversals not included in each age model are shown as black symbols. The plot for 30GGC includes two possible age models depending on which ages are included (see text). Water depths in each panel are rounded to nearest 100 m; exact depths are listed in Table 1.

Figure 3

Radiocarbon ages (squares) and benthic $\delta^{18}O$ results (circles) for the 30-120 cm depth interval in KNR159-5-78GGC. Both the ^{14}C ages and $\delta^{18}O$ results indicate the presence of disturbed sediment from 69-81 cm. Both proxies suggest the material originated from the 35-45 cm stratigraphic level. Also shown is the interval of $\delta^{13}C$ decline in 78GGC at the beginning of HS1. Note that the depth interval of this transition and the disturbed material do not coincide.

Figure 4

Radiocarbon-constrained $\delta^{18}O$ and $\delta^{13}C$ time series for the Brazil Margin spanning 1300 m to 2500 m water depth. Each panel includes stable isotopic results for individual foraminifera (circles), the average value at each stratigraphic level (thin line), the 2000-year running mean (thick line), and the standard error (dashed lines). Red symbols denote calendar ages for each core. The running mean at 2500 m water depth is calculated only between 13 and 25 kyr BP due to a lack of high resolution Holocene data. Isotopic values out of stratigraphic order (black squares) were not included in the time averages. At 1600 m water depth, benthic $\delta^{13}C$ values more than 0.4‰ lower than surrounding values were excluded from the time average. The age model shows clear evidence of disturbance in this interval, most likely due to burrowing (Figure 2). Boxes indicate intervals used for calculating mean HS1 (14.5-17.5 kyr BP) and LGM (19-23 kyr BP) values. Water depths in figures are rounded to nearest 100 m; exact depths are listed in Table 1.

Figure 5

A) 3-point running mean benthic $\delta^{13}C$ for 1800 m (black and grey lines) and 2100 m (green line) compared to the atmospheric $\delta^{13}C$ record from 0-25 kyr BP (red line)

(Schmitt et al., 2012) . Results at 2100 m are shifted by +0.1‰ to aid comparison with the record from 1800 m water depth. Two separate curves are shown for the 1800 m, including no change in the regional reservoir age correction (ΔR = 0 years; black line) and a ΔR of 400 years from 12-18 kyr BP (dark grey line). Triangles denote radiocarbon control points. Three separate curves are shown for EDC $\delta^{13}C$, including the spline fit from Schmitt et al. (2012) (thick red line), the raw data from Schmitt et al. (2012) smoothed using a 1500-year Gaussian filter (dashed red line), and the data from Schmitt et al. (2012) on the age model of Parrenin et al. (2013) smoothed using a 1500-year Gaussian filter (thin red line). The dashed red line shows that the Gaussian filter yields a time series very similar to the spline fit during the $\delta^{13}C$ decline at the beginning of HS1. B) Rate of $\delta^{13}C$ change (in ‰ per century) for the time series in panel A. The maximum rate of change for both Brazil Margin records occurs at 17.8 kyr BP, assuming a ΔR of 0 years. If ΔR was instead 400 years, the maximum rate of $\delta^{13}C$ decline occurs at 17.3 kyr BP. The maximum rate of change for the atmospheric record occurs from 16.9-17.3 kyr BP depending on the age model applied.

<u>Figure 6</u>

Cross-plots of $\delta^{13}C$ vs. $\delta^{18}O$ for the Brazil Margin. (A) LGM cross-plot, including data from Curry and Oppo (2005) above 3100 m water depth and Hoffman and Lund (2012) below 3100 m. The Southwest Atlantic was occupied by four distinct water masses, including Glacial Antarctic Bottom Water (GAABW), Glacial North Atlantic Intermediate Water (GNAIW), Glacial Antarctic Intermediate Water (GAAIW) and

Glacial Sub-Antarctic Mode Water (GSAMW). (B) HS1 cross-plot, including Brazil Margin data from 1300 m to 2500 m (this paper) and 3600 m to 3900 m (Hoffman and Lund, 2012). The latter points represent southern component water (SCW). Also shown is the estimated $\delta^{13}C$ and $\delta^{18}O$ range for northern component water (NCW) during HS1 (Zahn et al., 1997; Zahn and Stuber, 2002; Rickaby and Elderfield, 2005; Peck et al., 2007; Thornalley et al., 2010). The mid-depth Brazil Margin results plot above the mixing line between NCW and SCW. A similar pattern occurs when only data from the HS1 $\delta^{13}C$ minimum are used (not shown).

Figure 7

High resolution benthic stable isotopic records for 1800 m and 2100 m water depth at the Brazil Margin for the 15 to 20 kyr BP time interval. The time series are based on the average isotopic value at each stratigraphic level in the core. Triangles denote calendar-calibrated age control points.

Figure 8

Top) Radiocarbon-constrained benthic $\delta^{13}C$ time series for core 78GGC at 1800 m water depth on the Brazil Margin (red) and core M35003 at 1300 m water depth in the western Tropical Atlantic (black) (Zahn and Stuber, 2002). Results are plotted as 2000-year running mean values (solid lines) and ±1 SE (dotted lines). The original Zahn and Stuber (2002) age model for M35003 has been updated using CALIB 6.0 (http://calib.qub.ac.uk/calib/) and a ΔR of 0 ± 200 years (1σ).

Bottom) Same as top panel but for benthic foraminiferal $\delta^{18}O$.

Figure 9

Left-hand column) Vertical profiles of benthic foraminiferal $\delta^{13}C$ for the LGM (19-23 kyr BP; blue) and HS1 (red) in the North and South Atlantic. Solid red symbols are the average $\delta^{13}C$ for 14.5-17.5 kyr BP. Horizontal lines represent the one-sigma standard deviation and small vertical lines are the standard error. In most cases the standard error is smaller than the size of the triangle symbol. Open red symbols represent the average $\delta^{13}C$ during the HS1 $\delta^{13}C$ minima in each core. To improve clarity the standard deviation and standard error are not shown for the $\delta^{13}C$ minima. The South Atlantic profiles are based on data presented in this paper while the North Atlantic profiles are compiled from published records (Table 3). Right-hand column) Same as left-hand column except for benthic foraminiferal $\delta^{18}O$. Note that $\delta^{18}O$ results indicate there were two separate watermasses in the North and South Atlantic during HS1 while the $\delta^{13}C$ data suggest there was a single dominant watermass that spanned the entire basin.

References

Anderson, R. F., S. Ali, L. I. Bradtmiller, S. H. H. Nielsen, M. Q. Fleisher, B. E. Anderson, and L. H. Burckle (2009), Wind-Driven Upwelling in the Southern Ocean and the Deglacial Rise in Atmospheric CO2, *Science*, *323*(5920), 1443-1448.

Angulo, R. J., M. C. de Souza, P. J. Reimer, and S. K. Sasaoka (2005), Reservoir effect of the southern and southeastern Brazilian coast, *Radiocarbon*, *47*(1), 67-73.

Broecker, W. S., and E. Maier-Reimer (1992), The influence of air and sea exchange on the carbon isotope distribution in the sea, *Global Biogeochemical Cycles*, *6*(3), 315-320.

Charles, C. D., J. LynchStieglitz, U. S. Ninnemann, and R. G. Fairbanks (1996), Climate connections between the hemisphere revealed by deep sea sediment core ice core correlations, *Earth and Planetary Science Letters*, *142*(1-2), 19-27.

Curry, W. B., and D. W. Oppo (2005), Glacial water mass geometry and the distribution of delta C-13 of Sigma CO2 in the western Atlantic Ocean, *Paleoceanography*, *20*(1).

Curry, W. B., J. C. Duplessy, L. D. Labeyrie, and N. J. Shackleton (1988), Changes in the distribution of d13C of deep water CO2 between the last glaciation and Holocene, *Paleoceanography*, *3*, 317-341.

Dokken, T. M., and E. Jansen (1999), Rapid changes in the mechanism of ocean convection during the last glacial period, *Nature*, *401*(6752), 458-461.

Gherardi, J. M., L. Labeyrie, S. Nave, R. Francois, J. F. McManus, and E. Cortijo (2009), Glacial-interglacial circulation changes inferred from Pa-231/Th-230 sedimentary record in the North Atlantic region, *Paleoceanography*, *24*, 14.

Hoffman, J. L., and D. C. Lund (2012), Refining the stable isotope budget for Antarctic Bottom Water: New foraminiferal data from the abyssal southwest Atlantic, *Paleoceanography*, *27*.

Kroopnick, P. M. (1985), THE DISTRIBUTION OF C-13 OF SIGMA-CO2 IN THE WORLD OCEANS, *Deep-Sea Research Part a-Oceanographic Research Papers*, *32*(1), 57-84.

Lund, D. C., J. F. Adkins, and R. Ferrari (2011), Abyssal Atlantic circulation during the Last Glacial Maximum: Constraining the ratio between transport and vertical mixing, *Paleoceanography*, *26*, 19.

Marshall, J., and K. Speer (2012), Closure of the meridional overturning circulation through Southern Ocean upwelling, *Nature Geoscience*, *5*, 171-180.

McManus, J. F., D. W. Oppo, and J. L. Cullen (1999), A 0.5-million-year record of millennial-scale climate variability in the North Atlantic, *Science*, *283*(5404), 971.

Monnin, E., et al. (2004), Evidence for substantial accumulation rate variability in Antarctica during the Holocene, through synchronization of CO2 in the Taylor Dome, Dome C and DML ice cores, *Earth and Planetary Science Letters*, *224*(1-2), 45-54.

Neftel, A., H. Oeschger, J. Schwander, B. Stauffer, and R. Zumbrunn (1982), ICE CORE SAMPLE MEASUREMENTS GIVE ATMOSPHERIC CO2 CONTENT DURING THE PAST 40,000 YR, *Nature*, *295*(5846), 220-223.

Ninnemann, U. S., and C. D. Charles (1997), Regional differences in Quaternary Subantarctic nutrient cycling: Link to intermediate and deep water ventilation,

Paleoceanography, *12*(4), 560-567.
Oppo, D. W., and R. G. Fairbanks (1989), Carbon isotope composition of tropical surface water during the past 22,000 years, *Paleoceanography*, *4*, 333-351.
Oppo, D. W., and M. Horowitz (2000), Glacial deep water geometry: South Atlantic benthic foraminiferal Cd/Ca and delta C-13 evidence, *Paleoceanography*, *15*(2), 147-160.
Oppo, D. W., and W. B. Curry (2012), Deep Atlantic Circulation During the Last Glacial Maximum and Deglaciation, *Nature Education Knowledge*, *3*(4).
Ostermann, D. R., and W. B. Curry (2000), Calibration of stable isotopic data: An enriched delta O-18 standard used for source gas mixing detection and correction, *Paleoceanography*, *15*(3), 353-360.
Parrenin, F. et al., Synchronous change of atmospheric CO_2 and Antarctic temperature during the last deglacial warming, *Science, 339,* 1060-1063.
Peck, V. L., I. R. Hall, R. Zahn, and J. D. Scourse (2007), Progressive reduction in NE Atlantic intermediate water ventilation prior to Heinrich events: Response to NW European ice sheet instabilities? *Geochemistry Geophysics Geosystems*, *8,* 1.
Rickaby, R. E. M., and H. Elderfield (2005), Evidence from the high-latitude North Atlantic for variations in Antarctic Intermediate water flow during the last deglaciation, *Geochemistry Geophysics Geosystems*, *6*, 12.
Schmitt, J., et al. (2012), Carbon Isotope Constraints on the Deglacial CO2 Rise from Ice Cores, *Science*, *336*(6082), 711-714.
Sigman, D. M., and E. A. Boyle (2000), Glacial/interglacial variations in atmospheric carbon dioxide, *Nature*, *407*(6806), 859-869.
Sigman, D. M., M. P. Hain, and G. H. Haug (2010), The polar ocean and glacial cycles in atmospheric CO2 concentration, *Nature*, *466*(7302), 47-55.
Sortor, R. N., and D. C. Lund (2011), No evidence for a deglacial intermediate water Delta C-14 anomaly in the SW Atlantic, *Earth and Planetary Science Letters*, *310*(1-2), 65-72.
Spero, H. J., and D. W. Lea (2002), The cause of carbon isotope minimum events on glacial terminations, *Science*, *296*(5567), 522-525.
Thornalley, D. J. R., I. N. McCave, and H. Elderfield (2010), Freshwater input and abrupt deglacial climate change in the North Atlantic, *Paleoceanography*, *25*, 16.
Waelbroeck, C., J. C. Duplessy, E. Michel, L. Labeyrie, D. Paillard, and J. Duprat (2001), The timing of the last deglaciation in North Atlantic climate records, *Nature*, *412*(6848), 724-727.
Waelbroeck, C., L. C. Skinner, L. Labeyrie, J. C. Duplessy, E. Michel, N. V. Riveiros, J. M. Gherardi, and F. Dewilde (2011), The timing of deglacial circulation changes in the Atlantic, *Paleoceanography*, *26*, 10.
Zahn, R., and A. Stuber (2002), Suborbital intermediate water variability inferred from paired benthic foraminiferal Cd/Ca and delta C-13 in the tropical West Atlantic and linking with North Atlantic climates, *Earth and Planetary Science Letters*, *200*(1-2), 191-205.
Zahn, R., J. Schonfeld, H. R. Kudrass, M. H. Park, H. Erlenkeuser, and P. Grootes (1997), Thermohaline instability in the North Atlantic during meltwater events: Stable isotope and ice-rafted detritus records from core SO75-26KL, Portuguese margin, *Paleoceanography*, *12*(5), 696-71s0

Core	Latitude (°S)	Longitude (°W)	Water Depth (m)
36GGC	27° 31’	46°28’	1268
17JPC	27°42’	46°29’	1627
78GGC	27°29	46°20’	1820
33GGC	27°34’	46°11’	2082
42JPC	27°46’	46°38’	2296
30GGC	28°08’	46°04’	2500

Table 1. Locations and water depths of Brazil Margin cores used in this paper. All cores were retrieved during R/V Knorr cruise KNR159-5.

Endmember	$\delta^{13}C$	error	$\delta^{18}O$	error
GAAIW	0.4	0.1	4.3	0.1
GNAIW	1.4	0.1	4.2	0.1
GAABW	-0.2	0.2	4.9	0.1

Table 2a. Stable isotope values for LGM endmembers in the Atlantic. Endmember values for GAAIW and GNAIW are based on isotope data presented in Curry and Oppo (2005). Endmember values for GAABW are based on results from Hoffman and Lund (2012).

Water depth (m)	Mixture	LGM $\delta^{13}C$	LGM $\delta^{18}O$	% GAAIW or GAABW	%GNAIW	Est. $\delta^{18}O$	Observed-Estimated $\delta^{18}O$
1268	GAAIW:GNAIW	0.6	4.20	80	20	4.28	-0.08
1627	GAAIW:GNAIW	0.9	4.30	50	50	4.25	0.05
1820	GAABW:GNAIW	1	4.40	25	75	4.38	0.03
2082	GAABW:GNAIW	0.77	4.50	39	61	4.48	0.02
2296	GAABW:GNAIW	0.55	4.52	53	47	4.57	-0.05
2500	GAABW:GNAIW	0.46	4.60	59	41	4.61	-0.01

Table 2b. LGM proportions of SCW and NCW at the Brazil Margin. Proportions are estimated using $\delta^{13}C$ because of the large range in the endmember $\delta^{13}C$ values. The resulting proportions are then used to estimate the expected $\delta^{18}O$ at each water depth. The observed minus estimated $\delta^{18}O$ values are all less than 0.1‰, indicating that $\delta^{13}C$ acted as a conservative watermass tracer during the LGM.

Core	Location	Latitude (°N)	Longitude (°W)	Water Depth (m)	Reference
SO75-26KL	Iberian Margin	37°49'	09°30'	1099	Zahn et al., 1997
MD01-2461	SW Ireland Shelf	51°45'	12°55'	1153	Peck et al., 1997
M35003	Tobago Basin	12°5′	61°15′	1299	Zahn and Stuber, 2002
NEAP 4K	Björn Drift	61°30’	24°10’	1627	Rickaby and Elderfield, 2005
RAPiD-15-4P	South Iceland Rise	62°59′	17°35′	1237	Thornalley et al., 2010
RAPiD-15-4P	South Iceland Rise	62°18′	17°8′	2133	Thornalley et al., 2010
RAPiD-17-5P	South Iceland Rise	61°29′	19°32′	2303	Thornalley et al., 2010

Table 3. Locations and water depths of published high-resolution records from North Atlantic cores used in this paper.

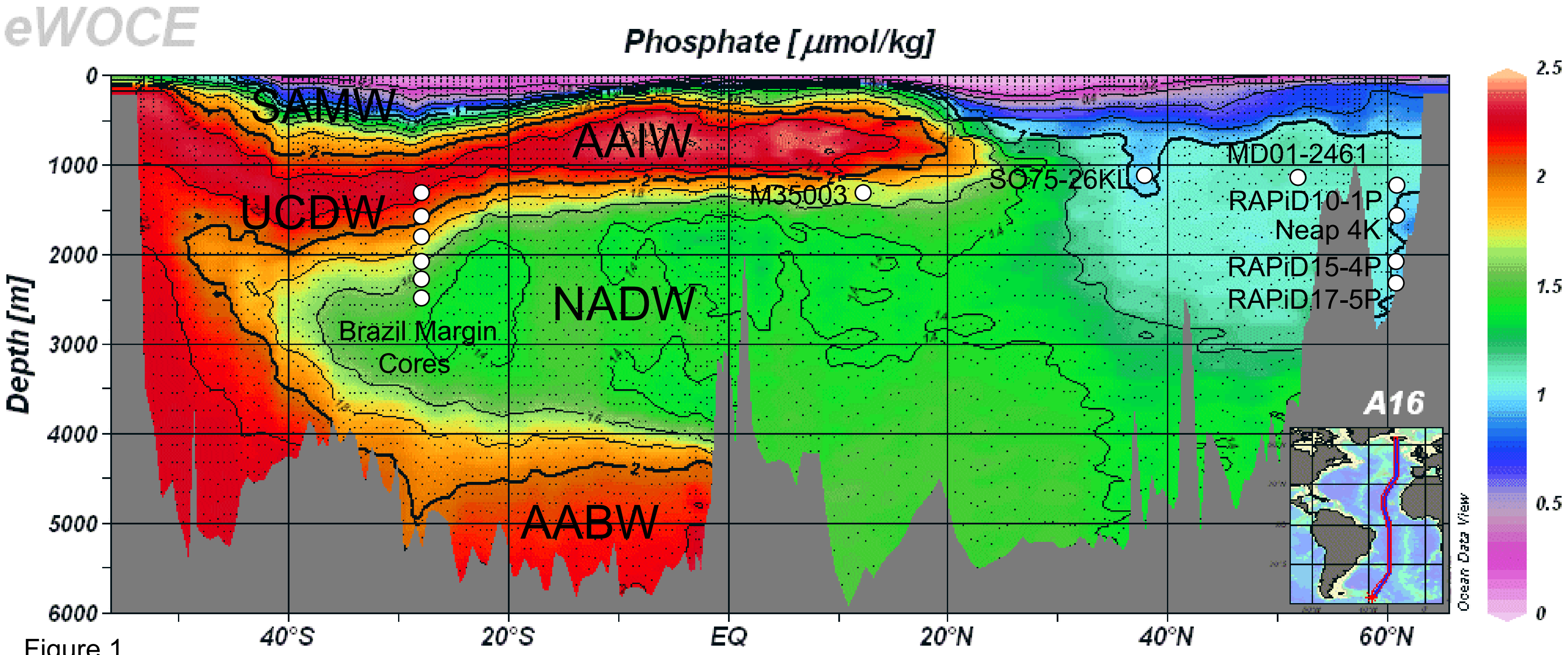
eWOCE
Phosphate [μmol/kg]
SAMW
AAIW
UCDW
NADW
AABW
Brazil Margin
Cores
M35003
SO75-26KL
MD01-2461
RAPiD10-1P
Neap 4K
RAPiD15-4P
RAPiD17-5P
A16
Depth [m]
0
1000
2000
3000
4000
5000
6000
40°S
20°S
EQ
20°N
40°N
60°N
2.5
2
1.5
1
0.5
0
Ocean Data View

Figure 1

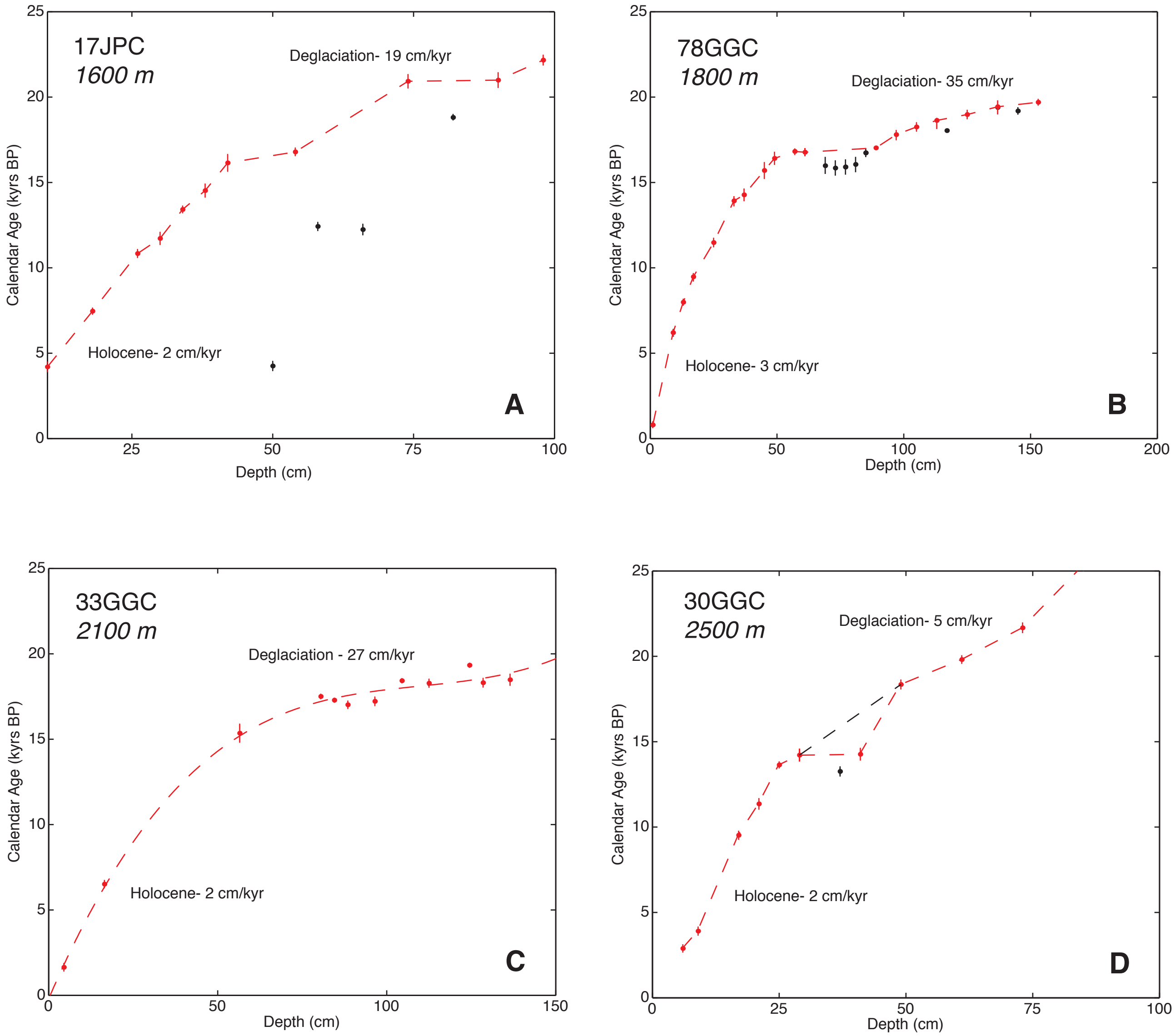
17JPC
1600 m
Deglaciation- 19 cm/kyr
Holocene- 2 cm/kyr
A
78GGC
1800 m
Deglaciation- 35 cm/kyr
Holocene- 3 cm/kyr
B
33GGC
2100 m
Deglaciation - 27 cm/kyr
Holocene- 2 cm/kyr
C
30GGC
2500 m
Deglaciation- 5 cm/kyr
Holocene- 2 cm/kyr
D
Calendar Age (kyrs BP)
Depth (cm)

Figure 2

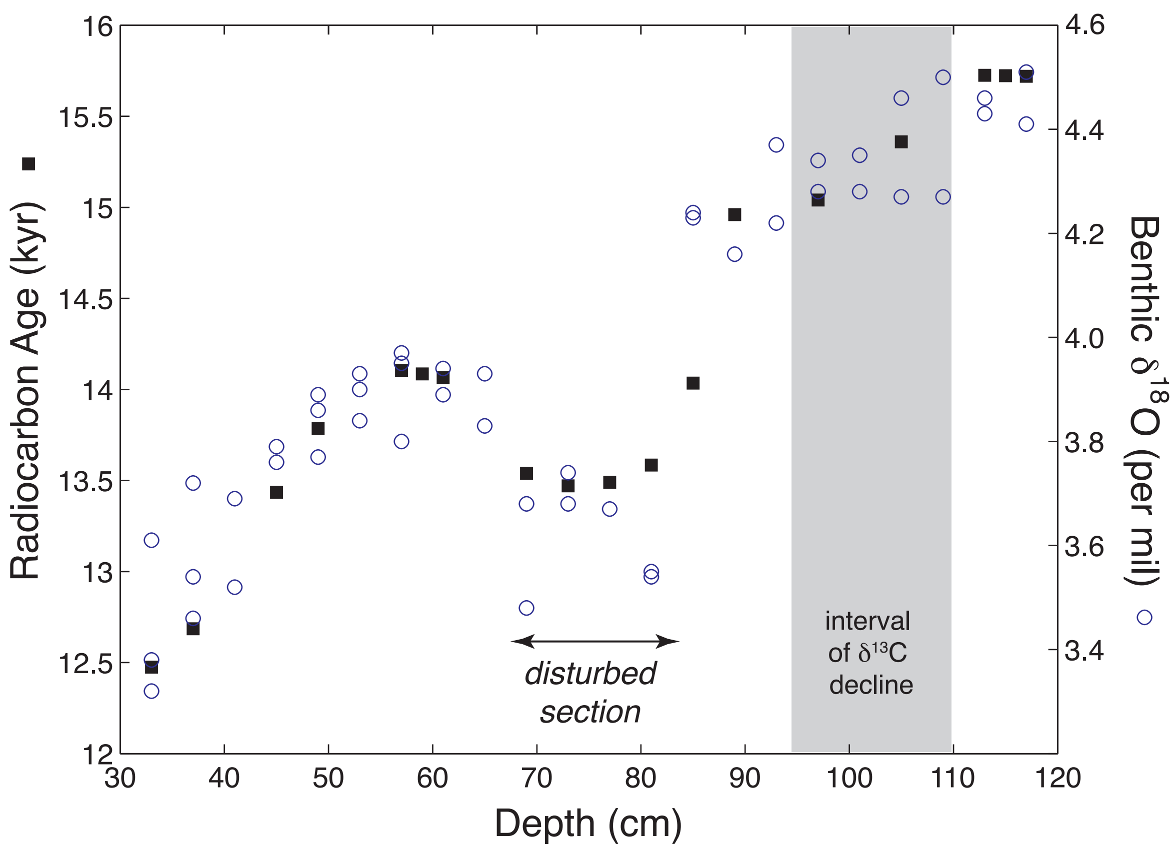

16
15.5
15
14.5
14
13.5
13
12.5
12
Radiocarbon Age (kyr)
4.6
4.4
4.2
4.0
3.8
3.6
3.4
Benthic δ18O (per mil)
30
40
50
60
70
80
90
100
110
120
Depth (cm)
disturbed section
interval of δ13C decline

Figure 3

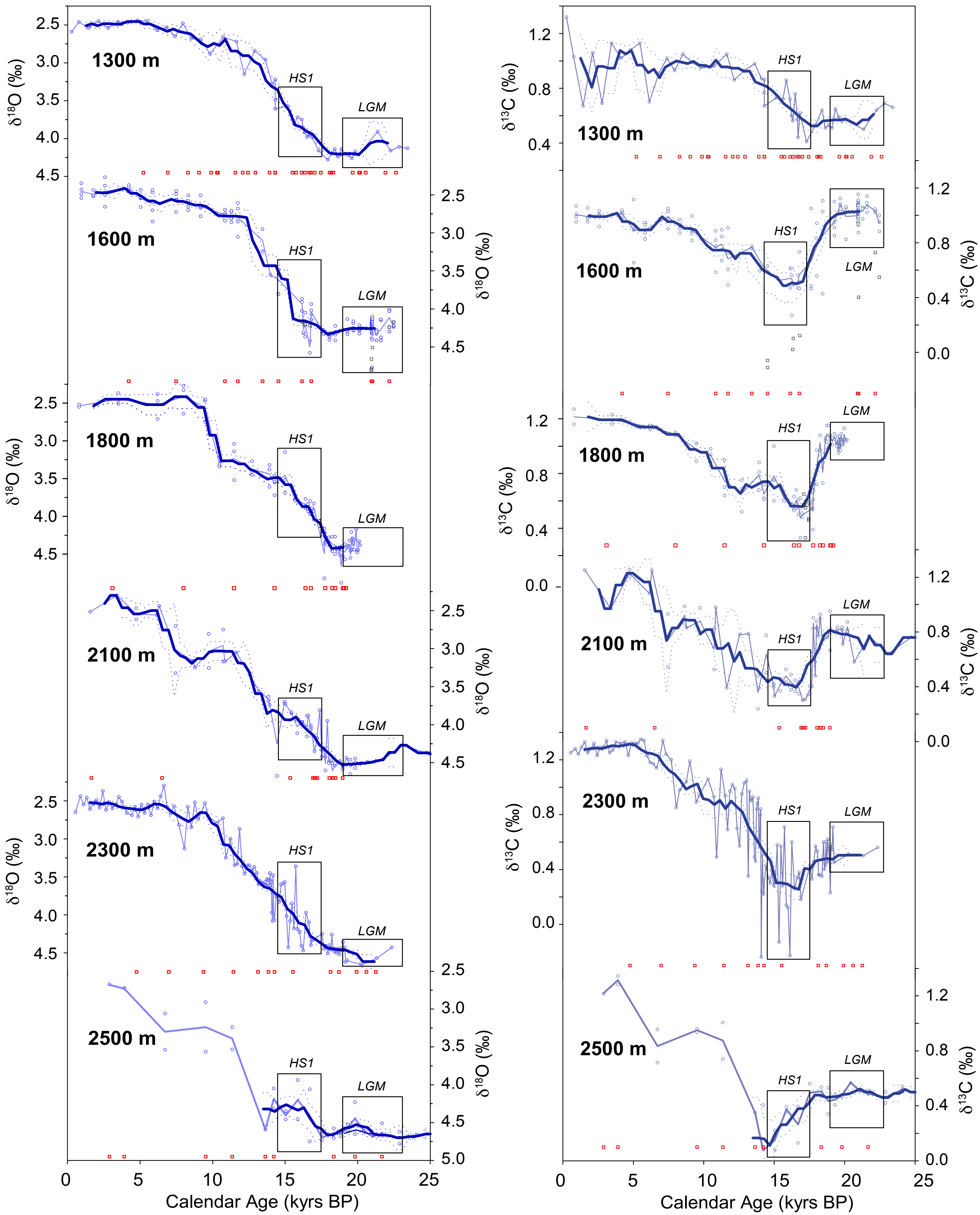

1300 m
1600 m
1800 m
2100 m
2300 m
2500 m
HS1
LGM
δ18O (‰)
δ13C (‰)
Calendar Age (kyrs BP)

Figure 4

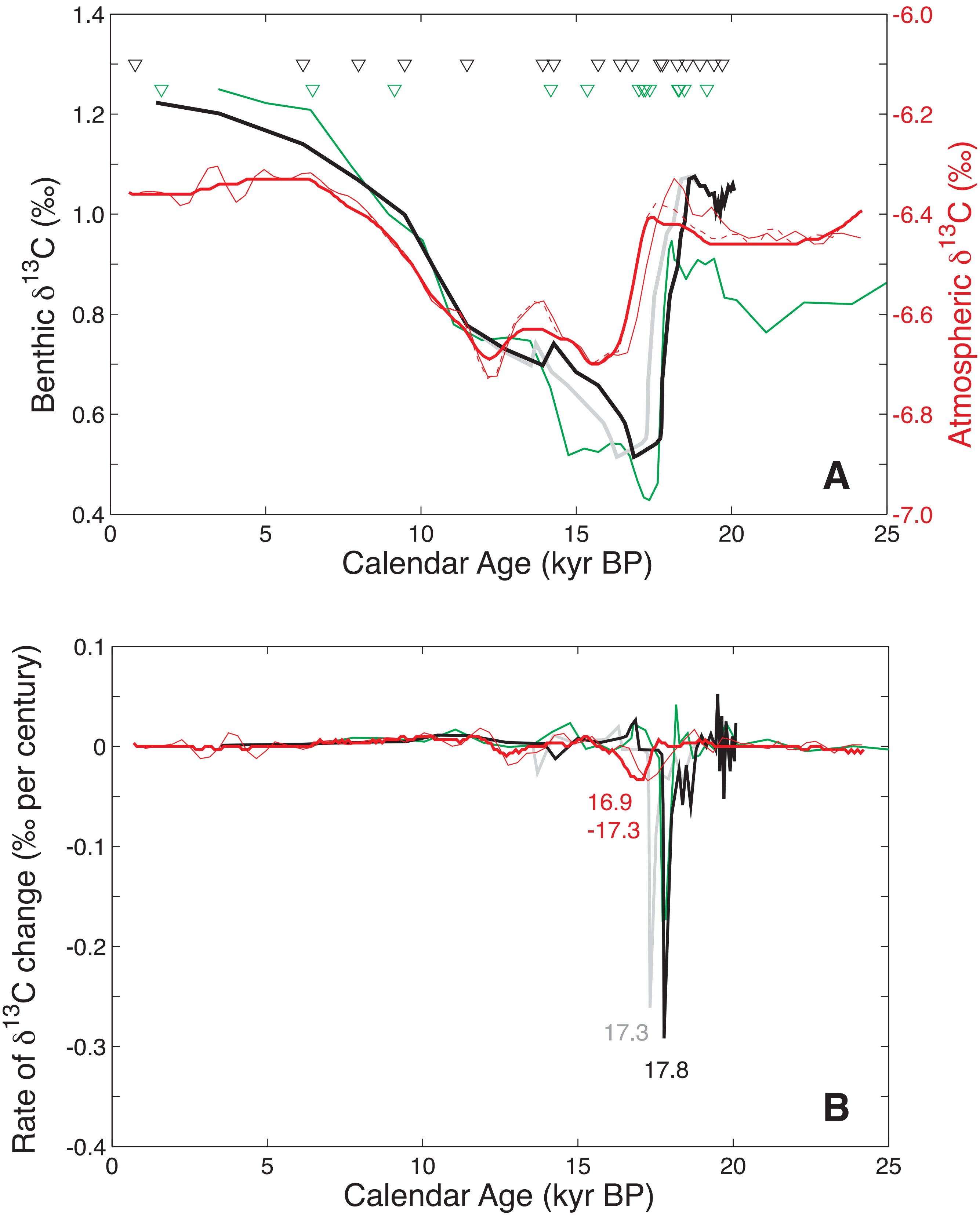
Benthic δ13C (‰)
Atmospheric δ13C (‰)
Calendar Age (kyr BP)
A
Rate of δ13C change (‰ per century)
16.9
-17.3
17.3
17.8
B

Figure 5

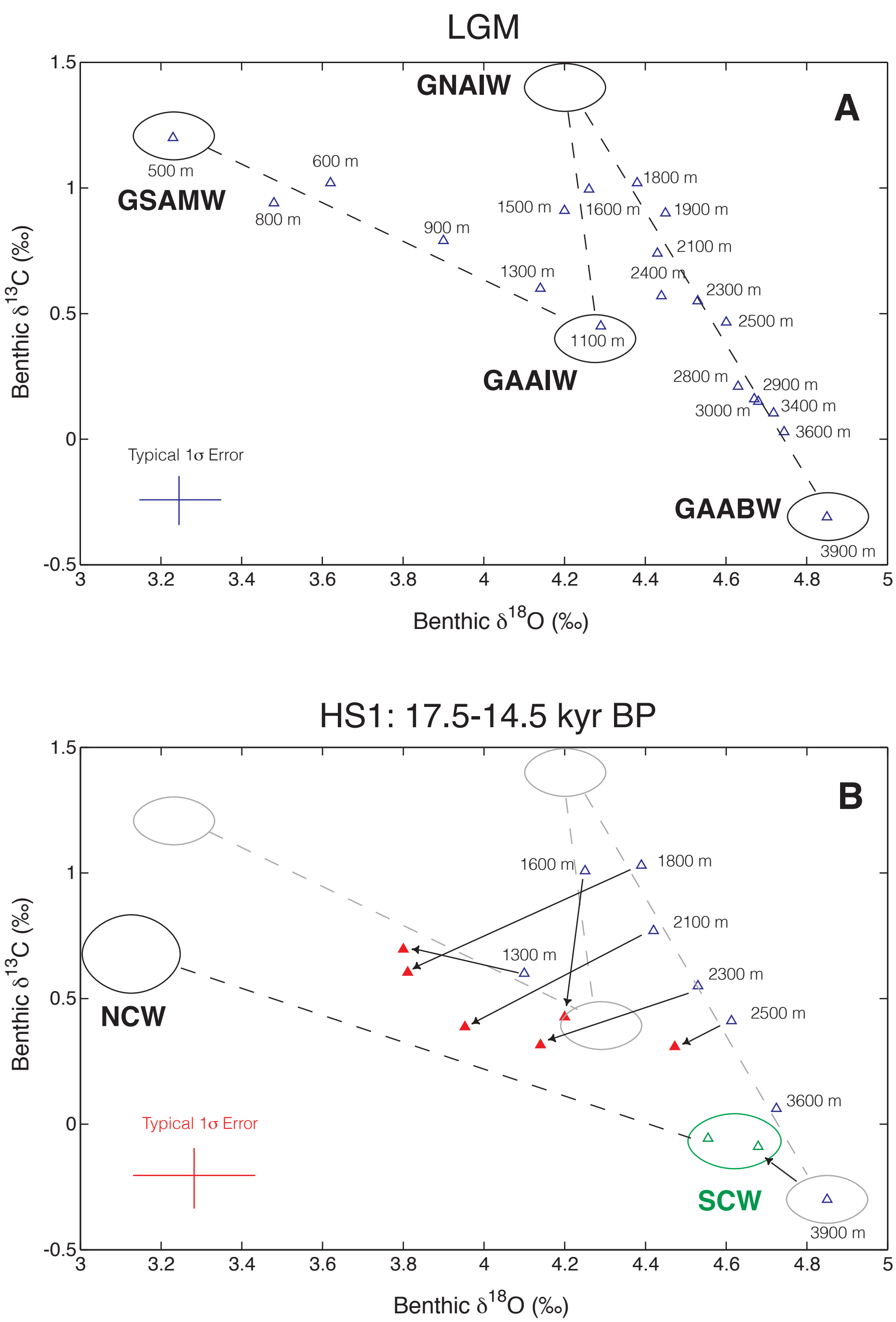

LGM
A
GNAIW
GSAMW
GAAIW
GAABW
500 m
600 m
800 m
900 m
1100 m
1300 m
1500 m
1600 m
1800 m
1900 m
2100 m
2400 m
2300 m
2500 m
2800 m
2900 m
3000 m
3400 m
3600 m
3900 m
Typical 1σ Error
Benthic δ13C (‰)
Benthic δ18O (‰)
HS1: 17.5-14.5 kyr BP
B
NCW
SCW
1600 m
1800 m
2100 m
1300 m
2300 m
2500 m
3600 m
3900 m
Typical 1σ Error
Benthic δ13C (‰)
Benthic δ18O (‰)

Figure 6

!

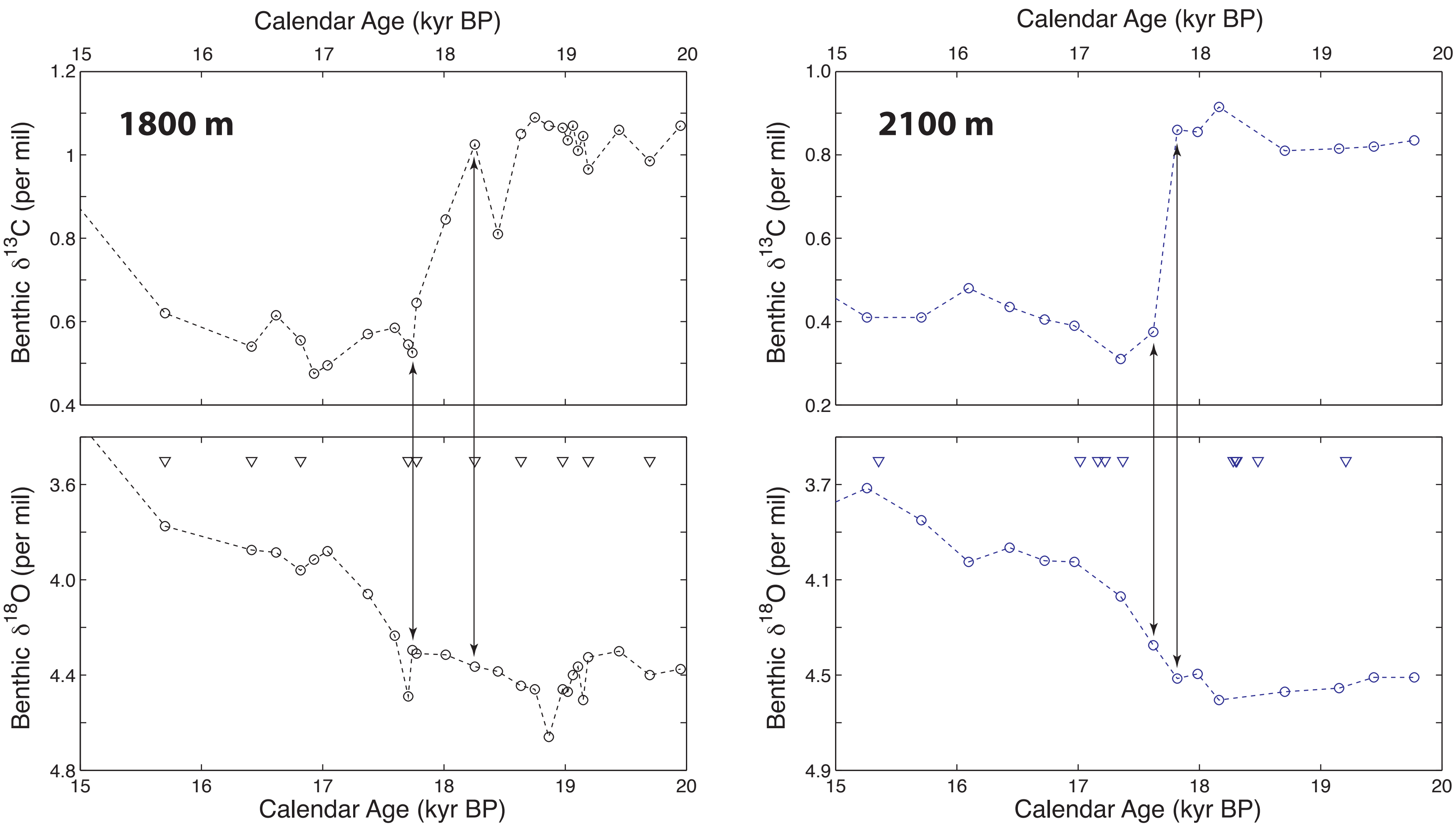

Calendar Age (kyr BP)
1800 m
Benthic $\delta^{13}C$ (per mil)
Benthic $\delta^{18}O$ (per mil)
Calendar Age (kyr BP)
Calendar Age (kyr BP)
2100 m
Benthic $\delta^{13}C$ (per mil)
Benthic $\delta^{18}O$ (per mil)
Calendar Age (kyr BP)

Figure 7

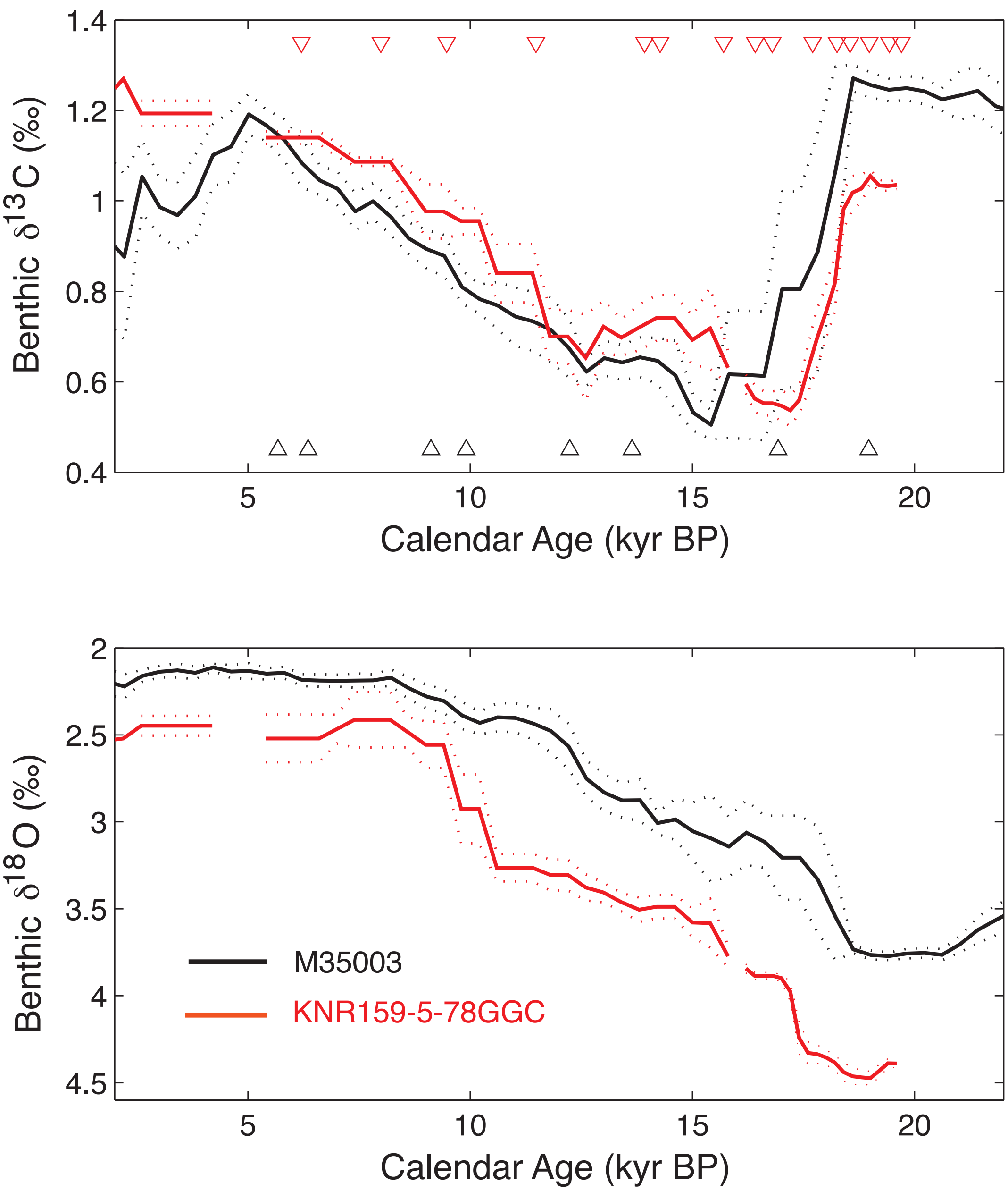

Benthic δ13C (‰)
1.4
1.2
1
0.8
0.6
0.4
5
10
15
20
Calendar Age (kyr BP)
Benthic δ18O (‰)
2
2.5
3
3.5
4
4.5
5
10
15
20
Calendar Age (kyr BP)
M35003
KNR159-5-78GGC

Figure 8

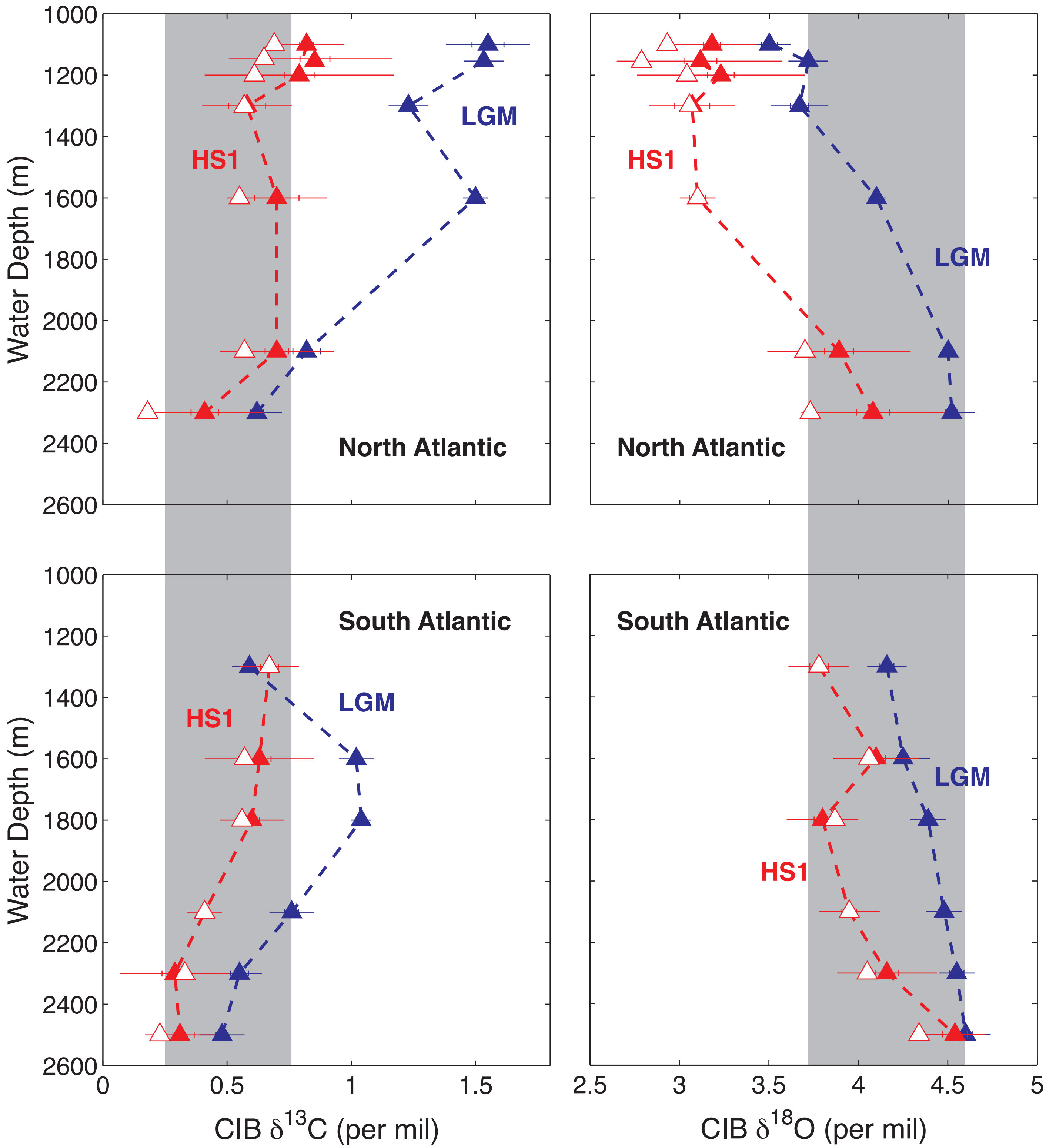

1000
1200
1400
1600
1800
2000
2200
2400
2600
Water Depth (m)
HS1
LGM
North Atlantic
South Atlantic
0
0.5
1
1.5
2.5
3
3.5
4
4.5
5
CIB δ13C (per mil)
CIB δ18O (per mil)

Figure 9